



Düzce University Journal of Science & Technology

Research Article

The Effect of Resolution and Watermark Strength on Multi-level DWT Image Watermarking

 Hüseyin Bilal MACİT^{a,*},

^a Department of Information Systems and Technologies, Bucak ZTYO, Burdur Mehmet Akif Ersoy University, Burdur, TURKEY

* Corresponding author's e-mail address: hbsmacit@mehmetakif.edu.tr

DOI: 10.29130/dubited.1246175

ABSTRACT

With the widespread use of the Internet and the decrease in storage costs, many media have been transferred to digital media. This situation reduces the security and reliability of digital media. Media producers use watermarking methods for copyright protection. This study focuses on wavelet transform, which is one of the frequency conversion methods for watermarking. The wavelet transform for the watermarking process is usually applied on one of the four subbands obtained in a single level. In this study, the watermarking process is carried out in a total of 12 sub-bands, including the 1st, 2nd and 3rd levels. In addition, a performance evaluation metric for digital image watermarking is presented. The evaluation is applied using 10 different watermark strength factors on 46 different image resolutions. The Ultra High-definition Demoiré Dataset is used for testing. The mathematical results obtained as a result of 22080 iterations are shown with tables and graphics, and the performance relations between the cover image resolution value and the sub-band selection are interpreted.

Keywords: Wavelet transform, Watermarking, Resolution

Çok Seviyeli DWT Görüntü Damgalamada Çözünürlük ve Damga Gücünün Etkisi

ÖZET

İnternetin yaygınlaşması ve depolama maliyetlerinin azalması ile çok sayıda medya dijital ortama taşınmıştır. Bu durum, dijital medyaların güvenliğini ve güvenilirliğini azaltmaktadır. Medya üreticileri, fikrî mülkiyet haklarının korunması için dijital damgalama yöntemlerini kullanırlar. Bu çalışma, damgalama için frekans dönüşüm yöntemlerinden biri olan dalgacık dönüşümüne odaklanmaktadır. Damgalama işlemi için dalgacık dönüşümü genellikle tek seviyede elde edilen dört alt banttan biri üzerinde uygulanır. Bu çalışmada damgalama işlemi, 1., 2. ve 3. seviye olmak üzere toplam 12 alt bantta gerçekleştirildi. Ayrıca dijital görüntü damgalanması için bir performans değerlendirme metriği sunuldu. Bu değerlendirme 46 farklı çözünürlük üzerinde 10 farklı damga dayanım faktörü kullanılarak uygulandı. Test için Ultra High-definition Demoiré Dataset kullanıldı. 22080 iterasyon sonucunda elde edilen matematiksel sonuçlar tablo ve grafikler ile gösterildi ve kapak görüntü çözünürlük değeri ile alt-bant arasındaki performans ilişkileri yorumlandı.

Anahtar Kelimeler: Dalgacık dönüşümü, Damgalama, Çözünürlük

I. INTRODUCTION

With the widespread use of electronic systems, data generation and transmission is getting easier day by day [1]. Ease of access to devices used to capture data such as photos, audio and video [2], improved image capture technologies of smart phones, new data compression techniques, new data storage methods and increasing personal data storage opportunities greatly increase the speed of digital media production of people. It is estimated that a total of 660 million digital photographs were created in 2013 and 1.2 trillion digital photographs were created in 2018 [3]. Rise Above Research, a consulting firm providing market research for the digital imaging industry, estimates that 1.4 trillion photos have been produced in 2021, and this number will grow by 100 million each year over the next 5 years [4]. The rapid increase in the number of digital images and the distribution of them in insecure environments [5,6] has led to the need to develop new image authentication techniques [7]. Digital images are also used for commercial purposes. This brings along the problems of copyright infringement [5]. The most effective method for copyright protection of a multimedia item is to use a watermark [1,6,7]. A watermarking technique is to embed visible or hidden information such as a logo [2], a signature, or a digital identifier into a media file and extract it when necessary [5]. In addition to copyright protection, digital watermarking methods are also used in application areas such as content verification, digital forensics, content identification and management, fingerprinting, tampering detection, broadcast monitoring and media file archiving [5]. Today, digital watermarking techniques are applied on digital video and digital audio media as well as digital images [2,6,8].

The two most important criteria for evaluating watermarking algorithms are; imperceptibility and robustness [6,7]. The robustness of the watermarking method shows the strength of the watermark against unauthorized attempts [8]. Robust watermarking methods are widely used for copyright protection and authentication [6]. Imperceptibility refers to the amount of alteration in a digital image after the embedding process [2]. Robustness and imperceptibility of a watermarking method are directly related to parameters such as the embedding and the extracting algorithm, characteristics of the watermark, and the strength factor. It is not possible for a watermarking method to be both very robust and very imperceptible at the same time [7].

Watermarking methods are examined in two classes according to the analog or digital processing of the multimedia element [8,9]. The watermarking methods applied in the digital environment are called the spatial domain watermarking methods. In the spatial domain, the watermark is embedded to the monochrome pixels of still images [5], audio samples, or pixel values of video frames. No transformation is applied to the main signal during watermark embedding. Spatial domain techniques are often used in authentication and tamper detection applications [2]. These techniques are highly vulnerable to image processing attacks, predictive analysis, and statistical analysis, and are less popular these days [10]. The watermarking methods applied in the analog environment are called the frequency domain watermarking methods. In these methods, the object to be watermarked is perceived as a signal. In other words, it is expressed in the frequency domain [11]. Today, most frequency domain watermarking methods are used because they provide better robustness [7,12]. These methods are resistant to forgery attacks such as clipping and adding noise, so that some parts of the watermark can be recovered after these attacks [13,14].

The basic numerical properties that define a digital image are expressed as color space, aspect ratio and resolution. Color space refers to the number of colors of the image and the luminance value for each color. Numerous color spaces are defined depending on the application. Color spaces are interrelated, so, an image in one color space can be transferred to another color space using the appropriate mathematical conversion formula [10]. Let I be a digital image with each pixel $x_{i,j}$.

$$I(c,r) = \{x_{i,j} | 1 \leq i \leq r, 1 \leq j \leq c\} \quad (1)$$

where c is the number of columns and r is the number of rows. The aspect ratio of an image is the ratio of its width to its height, and is expressed as $c:r$ for I . The total number of pixels of I is called

the resolution and is expressed in *cxr*. For example, the resolution value of an image consisting of 600 rows and 800 columns is 800x600 and the aspect ratio is 4: 3. As the resolution size increases (Figure 1), the amount of detail of the image increases.

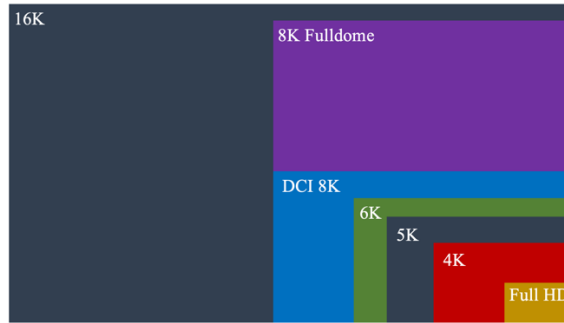


Figure 1. Some common broadcast resolutions

In the digital photo and video industry, resolution sizes are standardized by sensor or software manufacturers. Some of these standards are given in Table 1.

Table 1. Some of the display resolution standards

Standard	Resolution	Aspect Ratio	Standard	Resolution	Aspect Ratio
QQVGA	160 x 120	4:3	CGA	320 x 200	4:3
VGA	640 x 480	4:3	WVGA	800 x 480	5:3
WSVGA	1024 x 600	16:9	HD	1280 x 720	16:9
Full HD	1920 x 1080	16:9	DCI 2K	2048 x 1080	1.9:1
DCI 4K	4096 x 2160	1.9:1	6K	6016 x 3384	16:9
DCI 8K	8192 x 4320	1.9:1	16K	15360 x 8640	16:9

Video Graphics Array (VGA) is a video display controller device and a graphics standard first introduced in 1987 with the IBM PS/2 computer series [15]. Many low-resolution standards have been named, based on VGA. In 1990, IBM announced the XGA standard, which offers higher resolution [16]. In 2005, Digital Cinema Initiatives (DCI), one of the leading standards of the cinema industry, published the Digital Cinema System Specification [17]. This specification standardizes high resolution images such as DCI 2K, DCI 4K [18], and DCI 8K. Television and consumer media often uses 4K UHD (3840 × 2160) defined in SMPTE ST 2036-1 [19]. In 2019, Apple introduced the first 6K monitor called Pro Display XDR with a resolution of 6016x3384 [20]. The resolution of 7680x4320, called Ultra HD 8K, has been standardized by the International Telecommunication Union with the patent number ITU-R BT.2020-2 [21]. A 16K image is approximately 132 megapixels, 16 times the size of a 4K standard image. The world's first 16K display with a resolution of 15360×8640 was introduced by Innolux in Taiwan in 2018 [22]. At the beginning of 2023, 213 image standards and specifications are listed on Wikipedia [23].

Spatial domain image watermarking methods are resolution dependent. In these methods, as the number of pixels of the cover image decreases, the size of the watermark that can be used decreases. But, in the frequency domain, watermarking methods are independent of resolution. Also, the color space plays an important role in image watermarking [10]. Watermarking in the spatial domain is performed on a single-color space. In the frequency domain, the color space has no effect [12]. This article focuses on examining the effect of the resolution on watermarking performance in the frequency domain of color images. Discrete Wavelet Transform (DWT), which is one of the most applied methods for frequency domain transformation [5], has been applied in this paper. DWT-based watermarking methods have the advantages of multiple resolution, good energy compression, and imperceptible visual quality [24,25] and they are similar to theoretical models of the Human Visual System (HVS) [8]. The main purpose of this article is to compare the watermarking performance of sub-bands obtained by DWT at different resolutions. Four random images are selected from the Ultra High-definition Demoiréing Dataset [26] for the application. Test images are watermarked in 46

randomly selected resolution standards starting from QQVGA up to 16K. The robustness and imperceptibility results of watermarking on each resolution are demonstrated with a proposed hybrid metric score.

II. RELATED WORK

There are thousands of studies on watermarking in the literature. This section specifically mentions some of the sources cited in this article. Kahlessenane et.al. [27] presented a blind and robust watermarking technique that allows the integration of electronic patient records into computed tomography scanning. They applied a wavelet transform to the image, then made a topological rearrangement of the coefficients of the LL sub-bands using the ZigZag scanning method. Abdulrahman and Öztürk [5] proposed a new robust color image watermarking method based on Discrete Cosine Transform (DCT) and DWT. They divided RGB cover art into red, green and blue components, and applied DCT and DWT to each color component. Hemdan [9] offered a robust medical image watermarking approach based on Wavelet Fusion (WF), Singular Value Decomposition (SVD) and Multi-Level Discrete Wavelet Transform (M-DWT) with blending techniques. Liu et.al. [6] proposed a new image watermarking method based on DWT, Hessenberg Decomposition (HD) and SVD. They decomposed the cover image into a series of sub-bands with DWT and used the obtained coefficients as input for HD. They embedded the decomposed watermark into the cover image with the scaling factor. Ernawan et.al. [2] proposed an adaptive scaling factor based on selected DWT-DCT coefficients of its image content. The adaptive scaling factor was generated based on the role of selected DWT-DCT coefficients against the average value of DWT-DCT coefficients. Yin et.al. [12] proposed a novel watermarking scheme of embedding a scrambling watermark into the green component of the color image based on DWT-SVD. Al-Haj [8] describes an imperceptible and a robust combined DWT-DCT digital image watermarking algorithm. Kumar and Singh [7] proposed an adaptive color image watermarking scheme based on DWT by combining alpha blending and entropy concepts. Giri et.al. [28] provided a broader view as to how much work has been carried out so far and what are the different dimensions that have been taken into consideration to watermark color images using discrete wavelet transformation. Patvardhan et.al. [10] proposed a digital image watermarking technique to hide the relevant information in color YCbCr color space. Yu et.al [26] introduced a new digital watermarking encryption algorithm in which the watermarking information was based on the size of the image. Jing [1] proposed an image watermarking method based on the DCT algorithm, implemented it with Matlab, and proved the imperceptibility of the method with experimental results.

III. METHOD

Many methods have been proposed for transforming the image in the frequency domain. Some of the examples of these are DCT [1], (SVD) [29,30], Karhunen-Loeve transform [31,32], Hadamard transform [33,34], Contourlet transform [35,36]. DWT is the most used method of digital watermarking due to its success in spatial placement [8]. With DWT, the image is divided into frequency sub-bands. The watermark is embedded into one of these sub-bands with mathematical functions. Transforming a signal is actually just another way of representing that signal. Wavelet Transform provides time-frequency representation of the signal [37]. The transformation does not change the information contained in the signal; it just expands the signal into a wavelet domain. So, information that is not visible in the signal can be accessed. In other words, the signal is divided into different frequency components called wavelet coefficients using mathematical functions called wavelets [38]. Wavelets are special functions used as basal functions to represent signals [12]. Complex Wavelets, Daubechies Wavelet, Haar Wavelet, Bi-orthogonal Wavelets, Berkeley Wavelets, Wavelet Packets, Stationary Wavelets, Balanced Multi-wavelets, Non-tensor Wavelets, and Morphological Wavelets [28] are the wavelets generally used for watermarking applications.

Let the image to be watermarked be I and the watermark be W . Let the resolution of the I be $m \times n$. Since the image is a two-dimensional signal [39], a two-dimensional wavelet transform is applied. The two-dimensional wavelet transform is a one-dimensional analysis of a two-dimensional signal [37]. The wavelet chosen to perform the transformation in this paper is the Haar wavelet. Because the HVS is less sensitive to symmetry [28] and the Haar wavelet is a simple [27] and symmetrical wavelet. In the applied transformation, a window size is determined, then the signal is split into windows. The wavelet function is hovered over the windows sequentially. If the window and the wavelet are identical, the wavelet coefficient is calculated as $c = 1$ [40]. When the window width is kept large (at low frequency), the general outline of the signal is obtained with the slowly changing wavelet. When the window width is kept small (at high frequency), fast changing (detail) components of the signal are obtained. The important components of the image signal are obtained by passing through the Low Pass Filter (LPF) and the detail components are obtained by passing through the High Pass Filter (HPF). This process is called down-sampling (Equations 2 and 3).

$$LPF = \sum_i I(i)y[2I - i] \quad (2)$$

$$HPF = \sum_i I(i)a[2I - i] \quad (3)$$

Here, i indicates the index of the pixel being processed in the one-dimensional signal, $y[]$ and $a[]$ are high-pass and low-pass filter functions, respectively. The main purpose here is to separate the image from the noise. With DWT, the input signal is decomposed into four separate frequency sub-bands, each of size $(m/2) \times (n/2)$ corresponding to vertical, diagonal and horizontal details [27] respectively (Figure 2).

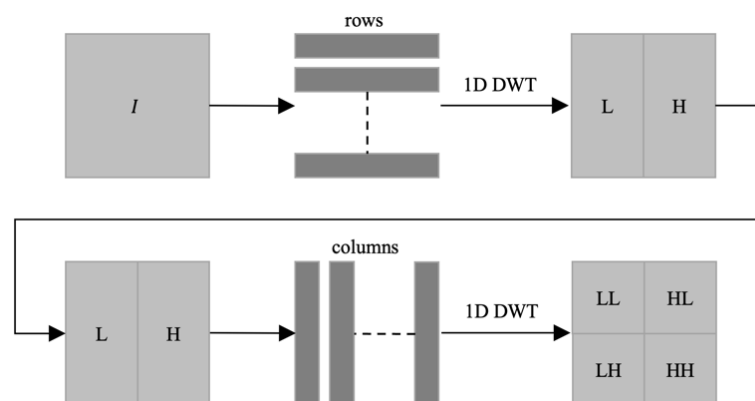


Figure 2. DWT frequency sub-bands

The low frequency (LL) sub-band contains more energy [27] and most of the information of the I is concentrated in this band [41,42]. This feature makes the LL sub-band suitable for robust watermarking [43]. LH and HL are vertical detail coefficients [2]. If a result in the middle of robustness and imperceptibility is desired, the watermark can be embedded in LH or HL sub-bands [44]. HH is the diagonal detail coefficient [2]. Embedding the watermark in high frequency coefficients means non-robust watermarking against JPEG compression [12]. Embedding the watermark in the HH sub-band offers robust watermarking against some attacks such as clipping, sharpening, contrast changing, histogram equalization, and gamma correction [45,46]. Figure 3 shows the sub-bands for the test image.

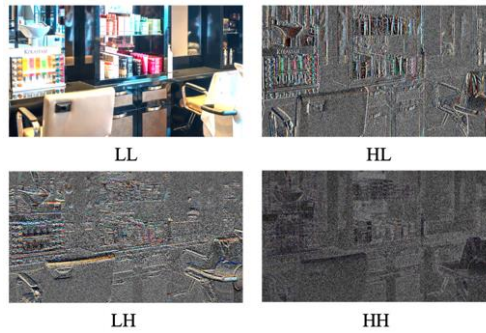


Figure 3. DWT frequency bands of test image

The watermark can be embedded in one or more of the LL, HL, LH, and HH sub-bands. For this, I is divided into sub-bands, W is set to the same row-column size as the sub-bands, then equation 4 is applied to the same sized sub-band and W .

$$SB_{I_w(i,j)} = (W_{(i,j)} \cdot \alpha) + (SB_{I(i,j)}) \quad (4)$$

In the equation, SB_I is the non-watermarked sub-band, and SB_{I_w} is it the watermarked one. i and j are the horizontal and vertical index information of the pixel. α is the watermark strength factor and it must be chosen between 0 and 1. When the α value is 0, the watermarking does not occur, when it is 1, the watermark is embedded by 50% of the sub-band. If the watermark is distinguishable by HVS after watermarking, it is called a visible watermark. Visible watermarks are generally embedded where detection of logo or label image is desired. If the watermark is not distinguishable by HVS, it is called an invisible watermark. Such watermarks are often embedded to identify the content owner [5]. α has a direct effect on the visibility of the watermark and the robustness of the watermarking. After embedding the watermark into the selected sub-band by applying Equation 4, the watermarked image I_w is reconstructed combining the embedded sub-band and the other three sub-bands (Equation 5) by Inverse DWT (IDWT).

$$I_w = \sum_{i=-\infty}^{\infty} (HPF[I]a[2W - I] + LPW[I]y[2W - I]) \quad (5)$$

The watermark extraction stage is the process of reading the watermark by subtracting it from the watermarked image [2]. The DWT method used in this study uses an unblind detector. The non-blind detector has prior information about the original image during the watermark extraction phase [27]. So, both I and I_w are required for watermark extraction. Sub-bands of I_w are obtained to extract the watermark, as in the watermarking phase. For this, I_w is treated as a one-dimensional signal, and it is passed through LPF and HPF as in equations 2 and 3, respectively. To extract the watermark, equation 6 is applied to the sub-band which carries the watermark.

$$W_e(i,j) = \frac{SB_{I_w(i,j)} - SB_{I(i,j)}}{\alpha} \quad (6)$$

Here, W_e is the extracted watermark. By applying DWT again to the 1st level sub-bands, it can be passed to the 2nd level sub-bands. When the k .level sub-band is reached, the resolution of the entire sub-band is $(m/2^k) \times (n/2^k)$. If the resolution of the image is much larger than the resolution of the watermark, the watermark can be embedded in the lower-level sub-bands by applying multiple DWTs. In this paper, the watermarking process on the sub-bands of the image is carried out by moving over the same sub-band(s) as shown in Figure 4. For example, to embed the watermark into the 3rd level HL sub-band (HL3), first the 1st level HL sub-band (HL1) is obtained. HL1 is again divided into sub-bands and 2nd level HL sub-band (HL2) is obtained. Then, HL2 is divided into sub-bands and 3rd level HL sub-band (HL3) is obtained. The watermark is resized and embedded in the HL3. Lastly, the IDWT operations are performed sequentially and I_w is obtained.

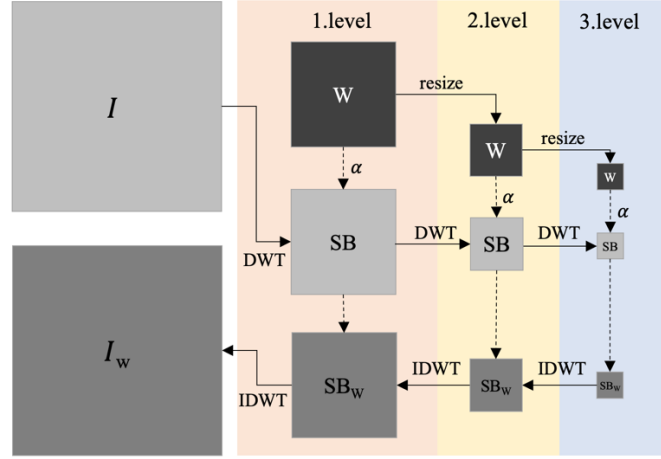


Figure 4. Flowchart of multi-level DWT watermarking

The two most important criteria for evaluating the performance of a watermarking algorithm are imperceptibility and robustness. The imperceptibility is measured by the amount of similarity between I and I_w , and the robustness is measured by the similarity between W and W_e . If these images are considered as signals, the alteration in the watermarked image can be calculated by the distance between two signals. In this paper, a hybrid similarity metric is calculated using Peak Signal to Noise Ratio (PSNR), Normalized Correlation (NC) and Structured Similarity Index (SSIM).

PSNR calculates the Gauss noise [47] between two signals using the Mean Squared Error (MSE). MSE is an old test to see whether two signals are how much similar [48]. Let I and S are two signals composed of N samples, x_i and y_i be samples of I and S , respectively. MSE is calculated in equation 7.

$$MSE(I, S) = \frac{1}{N} \sum_{i=1}^N (x_i - y_i)^2 \quad (7)$$

Let L is the peak value of I and S . PSNR is calculated by equation 8.

$$PSNR(I, S) = 10 \log_{10} \frac{L^2}{MSE(I, S)} = 10 \log_{10} \frac{255^2}{MSE(I, S)} \quad (8)$$

Here, the peak value is the maximum numerical value of a pixel. The maximum color value a pixel can hold for a 24-bit color image is 255. If two signals are the same, $PSNR = \infty$. $PSNR > 40$ is calculated if the two signals are structurally close to each other. However, PSNR is a mathematical approach and is not directly related to HVS. In signal processing, one of the techniques used to measure the similarity of two signals is cross-correlation. Since images are two-dimensional signals, two-dimensional correlation analysis can measure the similarity of two images. The correlation coefficient is calculated by shifting two images of $m \times n$ size over each other $m \cdot n$ times so that all pixels pass over each other. Equation 9 calculates the NC between the $m \times n$ sized cover image and the watermarked image.

$$NC(I, S) = \frac{\sum_m \sum_n (I - \bar{I})(S - \bar{S})}{\sqrt{(\sum_m \sum_n (I - \bar{I})^2)(\sum_m \sum_n (S - \bar{S})^2)}} \quad (9)$$

PSNR and NC are suitable for structural computation but they are not close to HVS. SSIM measurement is performed to obtain results close to HVS. To calculate SSIM (equation 10), images are decomposed into luminance component l , contrast component c , and structure component s [24].

$$SSIM(I, S) = l(I, S)^\alpha \cdot c(I, S)^\beta \cdot s(I, S)^\gamma \quad (10)$$

α , β , and γ are the three parameters used to adjust the importance of each of the three components. If the two images are identical, the SSIM value of 1 is calculated [47]. In this paper, a hybrid similarity score, which is the multiply of PSNR, NC, and SSIM, (Equations 11, 12) is proposed to measure the robustness and imperceptibility of watermarking in DWT sub-bands.

$$Ro = PSNR(W, W_e).NC(W, W_e).SSIM(W, W_e) \quad (11)$$

$$Im = PSNR(I, I_w).NC(I, I_w).SSIM(I, I_w) \quad (12)$$

Here, Ro refers to the robustness and Im refers to imperceptibility of the watermarking method.

IV. RESULTS AND CONCLUSIONS

In this paper, images 40, 199, 206 and 231 in the Ultra High-definition Demoiré Dataset [26] were used as test1, test2, test3, and test4 images, respectively (figure 5). The fact that the histogram characteristics of the selected test images are not similar to each other is important for the reliability of the results of the study.

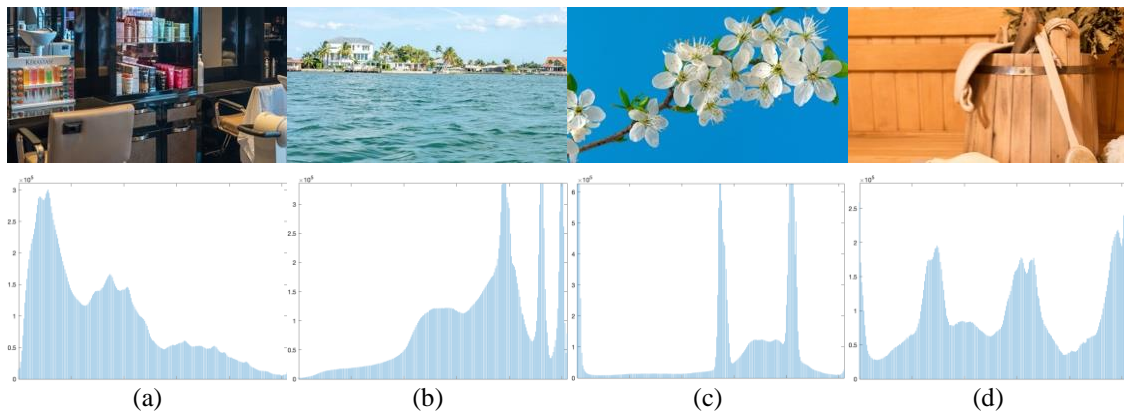


Figure 5. (a) test1 (b) test2 (c) test3 (d) test4 images and their histograms

A monochrome logo image was used as a watermark (figure 6).



Figure 6. Watermark

Test images were watermarked with the 46 different resolution standards shown in table 2. Ten different α values were used as $\{\alpha \in 0.01, 0.1, \dots, 1\}$. Each test image was watermarked with these parameters in the 1st, 2nd, and 3rd level LL, LH, HL and HH sub-bands. That is, a total of 22080 iterations were performed for the 4 test images. After each iteration, Ro and Im values were calculated and saved in Ro_{SB} and Im_{SB} matrices for the relevant sub-band, respectively. The average of these matrices was saved in the $Ro_{\mu SB}$ and $Im_{\mu SB}$ matrices for each sub-band. Table 2 shows the maximum and minimum robustness and imperceptibility values in $Ro_{\mu SB}$ and $Im_{\mu SB}$ matrices.

Table 2. Maximum and minimum of robustness and imperceptibility values of the mean results of test images with multi-level sub-band watermarking.

Standard	Resolution	min($I_{m_{\mu}}$)			max($I_{m_{\mu}}$)			min(Ro_{μ})			max(Ro_{μ})		
		sb	α	Value	sb	α	Value	sb	α	Value	sb	α	Value
QQVGA	160x120	LL3	0.91	0.84447	HH3	0.01	21.5308	HH1	0.01	-0.0650	LL1	0.31	0.38867
HQVGA	240x160	LL3	0.91	0.79407	HH3	0.01	23.4684	LH1	0.01	-0.0731	LL1	0.31	0.53059
CGA	320x200	LL3	0.91	0.73006	HH3	0.01	25.0289	LH1	0.01	-0.0783	LL1	0.21	0.63342
QVGA	320x240	LL3	0.91	0.69643	HH3	0.01	25.9791	HL1	0.01	-0.0827	LL1	0.21	0.70607
WQVGA	432x240	LL3	0.91	0.68613	HH3	0.01	26.5256	HL1	0.01	-0.082	LL1	0.21	0.71877
CGA	640x200	LL3	0.91	0.70624	HH3	0.01	25.9582	HL1	0.01	-0.0724	LL1	0.21	0.65205
HVGA	480x320	LL3	0.91	0.67334	HH3	0.01	28.3424	HL1	0.01	-0.0869	LL1	0.21	0.78889
VGA	640x480	LL3	0.91	0.61042	HH3	0.01	31.5342	HL1	0.01	-0.0885	LL1	0.21	0.84758
SVGA	800x600	LL3	0.91	0.56893	HH3	0.01	33.604	HL1	0.01	-0.0845	LL1	0.21	0.86815
PAL	1024x576	LL3	0.91	0.55742	HH3	0.01	33.8232	HL1	0.01	-0.0825	LL1	0.11	0.87293
DVGA	960x640	LL3	0.91	0.5633	HH3	0.01	34.5091	HL1	0.01	-0.079	LH1	0.91	0.91636
XGA	1024x768	LL3	0.91	0.53554	HH3	0.01	36.0028	HL1	0.01	-0.0694	LL1	0.11	0.92035
WXGA	1280x720	LL3	0.91	0.53074	HH3	0.01	35.9732	HL1	0.01	-0.0735	LH1	0.91	1.4853
WXGA	1280x768	LL3	0.91	0.52589	HH3	0.01	36.5044	HL1	0.01	-0.0677	LH1	0.91	1.4857
WXGA	1280x800	LL3	0.91	0.51977	HH3	0.01	36.8289	HL1	0.01	-0.0668	LH1	0.81	1.4858
SXGA	1280x960	LL3	0.91	0.50063	HH3	0.01	38.2496	HL1	0.01	-0.0444	LH1	0.91	1.4873
WXGA+	1440x900	LL3	0.91	0.43738	HH3	0.01	37.8929	HL1	0.01	-0.0564	LH1	0.71	1.9318
SXGA	1280x1024	LL3	0.91	0.4869	HH3	0.01	38.7471	HL1	0.01	-0.0398	LH1	0.91	1.4876
HD+	1600x900	LL3	0.91	0.43188	HH3	0.01	38.0892	HL1	0.01	-0.056	LH1	0.61	1.5199
1080i	1440x1080	LL3	0.91	0.48754	HH3	0.01	39.4644	HL2	0.01	-0.0382	LH1	0.71	1.9337
UXGA	1600x1200	LL3	0.91	0.46633	HH3	0.01	40.669	HL2	0.01	-0.0353	LH1	0.61	1.5217
DCI 2K	2048x1080	LL3	0.91	0.46817	HH3	0.01	40.1364	HL2	0.01	-0.034	LL1	0.11	0.97712
Full HD+	1920x1280	LL3	0.91	0.44585	HH3	0.01	41.6166	HL2	0.01	-0.0368	LL1	0.11	0.98734
TXGA	1920x1400	LL3	0.91	0.43479	HH3	0.01	42.3666	HL2	0.01	-0.0345	LL1	0.11	0.99931
QXGA	2048x1536	LL3	0.91	0.42599	HH3	0.01	43.3559	HL2	0.01	-0.0335	HL1	0.61	1.1374
WQHD	2560x1440	LL3	0.91	0.41618	HH3	0.01	43.0006	HL2	0.01	-0.0317	HL1	0.61	1.0616
WQXGA	2560x1600	LL3	0.91	0.40528	HH3	0.01	43.9754	HL2	0.01	-0.031	HL1	0.61	1.197
QSXGA	2560x2048	LL3	0.91	0.37415	HH3	0.01	46.3237	HL2	0.01	-0.0253	HL1	0.31	1.5277
WQXGA+	3200x1800	LL3	0.91	0.38052	HH3	0.01	45.2008	HH1	0.01	-0.055	HL1	0.61	1.2217
UW4K	3840x1600	LL3	0.91	0.3856	HH3	0.01	44.0789	HH1	0.01	-0.0572	HL1	0.61	1.1974
4K UHD-1	3840x2160	LL3	0.91	0.35293	HH3	0.01	47.0685	HH1	0.01	-0.0546	HL1	0.31	1.7291
WQUXGA	3840x2400	LL3	0.91	0.34003	HH3	0.01	48.2521	HH1	0.01	-0.0506	HL1	0.31	2.0277
UW5K	5120x2160	LL3	0.91	0.34084	HH3	0.01	47.1135	HH1	0.01	-0.0541	HL1	0.31	1.7296
HXGA	4096x3072	LL3	0.91	0.31114	HH3	0.01	50.2408	HH1	0.01	-0.0472	HL1	0.31	2.4902
5K	5120x2880	LL3	0.91	0.30969	HH3	0.01	50.2176	HH1	0.01	-0.0455	HL1	0.31	2.7514
WHXGA	5120x3200	LL3	0.91	0.29886	HH3	0.01	50.7446	HH1	0.01	-0.0449	HL1	0.11	2.1595
HSXGA	5120x4096	LL3	0.91	0.27866	HH3	0.01	52.717	HH1	0.01	-0.0389	HL1	0.31	1.4547
6K	6016x3384	LL3	0.91	0.28892	HH3	0.01	51.3585	LH1	0.01	-0.0457	HL1	0.21	2.5458
WHSXGA	6400x4096	LL3	0.91	0.27006	HH2	0.01	52.8571	LH1	0.01	-0.0443	HL1	0.31	1.4548
HUXGA	6400x4800	LL3	0.91	0.26498	HH2	0.01	53.4224	LH1	0.01	-0.0432	HL2	0.21	2.9734
8K UHD-2	7680x4320	LL3	0.91	0.26264	HH2	0.01	53.4889	LH1	0.01	-0.0469	HL1	0.31	1.5027
WHUXGA	7680x4800	LL3	0.91	0.2593	HH2	0.01	53.5158	LH1	0.01	-0.046	HL2	0.21	2.9752
DCI 8K	8192x4320	LL3	0.91	0.26083	HH2	0.01	53.5146	LH1	0.01	-0.0466	HL1	0.31	1.5027
UW10K	10240x4320	LL3	0.91	0.25487	HH2	0.01	53.575	LH1	0.01	-0.0461	HL1	0.31	1.5027
8K FullDome	8192x8192	LL3	0.91	0.24665	HH2	0.01	53.7432	LH1	0.01	-0.0455	LL1	0.11	1.0386
16K	15360x8640	LL3	0.91	0.23324	HH3	0.01	53.83	LH1	0.01	-0.0441	LL1	0.11	1.0398

The worst imperceptibility value was measured by watermarking the LL3 sub-band with high strength factor at all resolutions. I and I_w diverged from each other as the amount of resolution increased in the LL3 sub-band. The best imperceptibility was measured in the high-level sub-bands. High imperceptibility value was calculated with low strength factor in the sub-band HH2 at low resolutions and HH3 sub-band at high resolutions. Both of the worst and the best robustness values were measured in the 1st and 2nd level sub-bands. Watermark robustness is average in all the level 3 sub-bands. The robustness values in the 1st and 2nd level sub-bands vary according to the resolution and the histogram characteristic of the image. Figure 7 shows the estimated (a) worst imperceptibility, (b) best imperceptibility, (c) worst robustness and (d) best robustness results for test1 image based on the average values shown in Table 2.

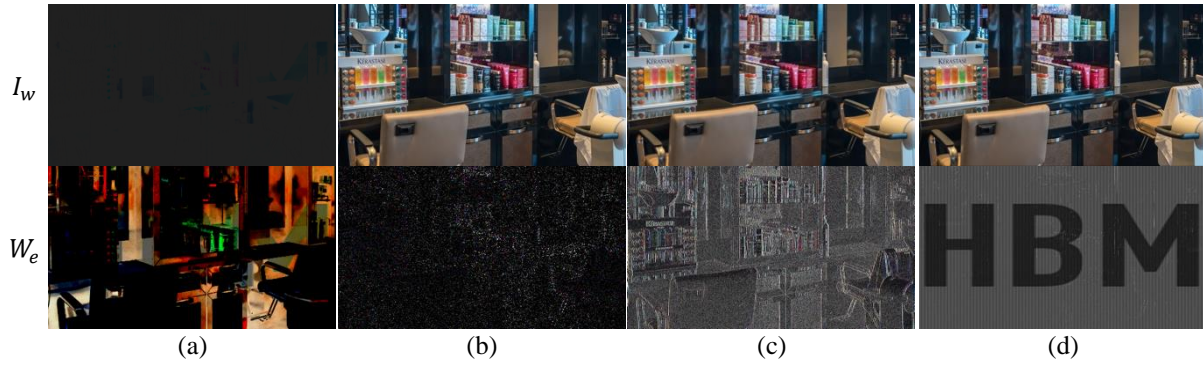


Figure 7. (a) 16K image watermarked in LL3 with $\alpha = 0.91$ (b) 16K image watermarked in HH3 with $\alpha = 0.01$ (c) VGA image watermarked in HL1 with $\alpha = 0.01$ (d) HUXGA image watermarked in HL2 with $\alpha = 0.21$

Figure 8 shows the surface plots of the imperceptibility, watermark strength, and pixel count for the Im_{μ} matrix. It is clear that the strength value only visibly affects the imperceptibility in the HL sub-band. In other sub-bands, the watermark strength does not affect the imperceptibility much. Watermarking into LL sub-bands is unsuccessful in imperceptibility, regardless of sub-band, watermark strength, and pixel count. In the HH and LH sub-bands, resolution up to 2 million pixels at 1st level DWT has no visible effect on imperceptibility. However, as the number of pixels increase in the 2nd and 3rd level sub-bands, the imperceptibility increases.

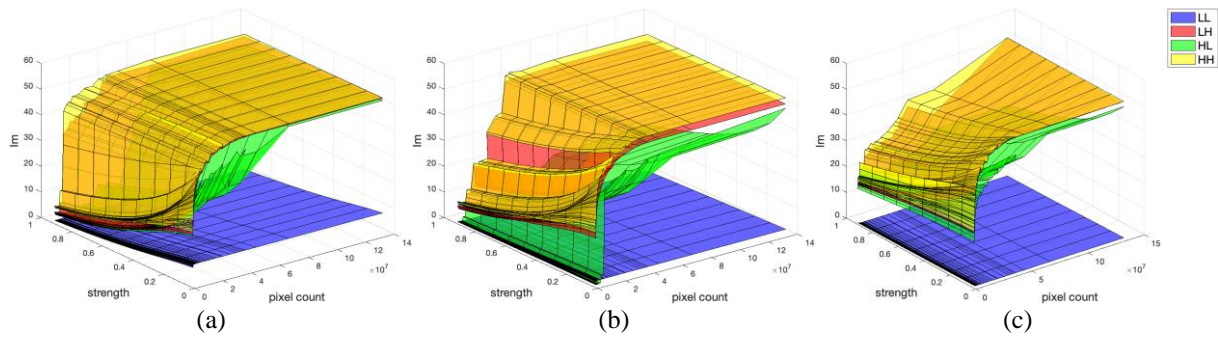


Figure 8. (a) Im_{μ} in 1st level sub-bands (b) Im_{μ} in 2nd level sub-bands (c) Im_{μ} in 3rd level sub-bands

Figure 9 shows the surface plots of the robustness, watermark strength, and pixel count for the Ro_{μ} matrix. Accordingly, more robust watermarking occurs in the LH sub-bands at low resolutions. At medium resolutions, on the other hand, more robust watermarking is achieved in the HL sub-band. At high resolutions, the LL sub-bands results with more robust watermarking. An increase in the watermarking strength increases the robustness in the LL1 and HL3 sub-bands, but decreases it in the LL1 sub-band.

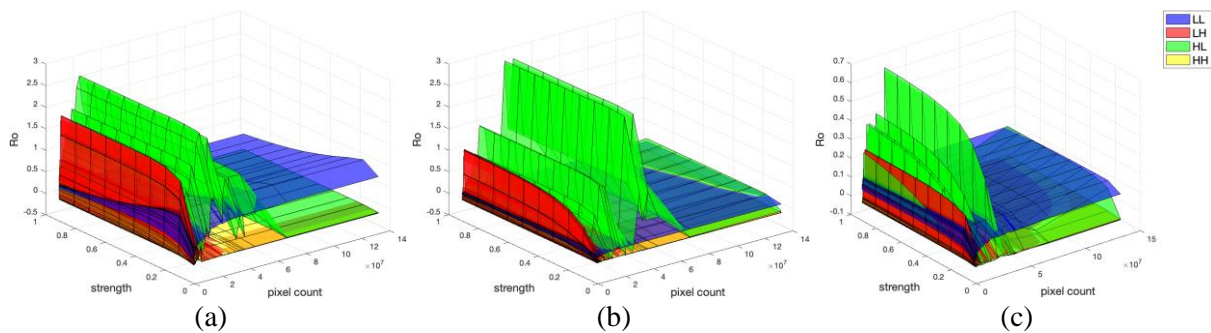


Figure 9. (a) Ro_{μ} in 1st level sub-bands (b) Ro_{μ} in 2nd level sub-bands (c) Ro_{μ} in 3rd level sub-bands

There are many studies in the literature on DWT watermarking or the technique of combining DWT and another watermarking technique. However, most of these studies focused on LL sub-bands. Few

studies use blend techniques combining two or more sub-bands. Also, few studies have compared performance between sub-bands. Table 3 shows the sub-band comparison results of some papers in the literature. As it is clearly seen in the table, there is no standard comparison metric.

Table 3. Literature comparison.

Paper	Test cover image(s)	Metric result(s) achieved	Sub-band			
			LL	LH	HL	HH
[27]	512x512 medical image database (computerized tomography scan)	Energy distribution of sub-bands.	99.9636%	0.0272%	0.0055%	0.0036%
[8]	Lena image	NC values after 0.4 Fausain noise attack	NaN	NaN	0.660	0.652
[49]	Lena image	Diagonal entries (singular values)	64.462	313	586	204
[50]	60 test images from 512x512 to 3840x2160 resolution	$T_{S_n,l}$ and $T_{S_n,h}$ (low and high energy or energy variance threshold values)	$T_{S_n,l} = 1.5$ $T_{S_n,h} = 2.5$	$T_{S_n,l} = 2$ $T_{S_n,h} = 8$	$T_{S_n,l} = 2$ $T_{S_n,h} = 8$	$T_{S_n,l} = 2$ $T_{S_n,h} = 8$
[51]	Lena image	NC between extracted and original watermark	0.9997	0.9391	0.9526	1.0154
[52]	Unspecified	PSNR of watermarked video (2-level DWT)	34.65	50.12	48.19	47.92
[53]	Unspecified	PSNR values of different sub-bands under different embedding intensities with the capacity of 128x128 resolution ($\alpha = 0.01$)	102.2821	78.7027	64.0317	57.4745

In this study, the watermarking performance was measured in 12 different sub-bands of DWT for 3 levels. Results were evaluated with a multi-criteria hybrid metric. In summary, it can be said that the robustness and imperceptibility criteria of the watermarking method do not depend only on the selected sub-band. The resolution of the image to be watermarked is as important a criterion as choosing the right sub-band.

V. REFERENCES

- [1] W.H. Jing, "A DCT domain image watermarking method based on Matlab," Int. J. Adv. Netw. Monit. Control, vol. 2, no. 2, pp. 38-45, 2017.
- [2] F. Ernawan, D. Ariatmanto and A. Firdaus, "An improved image watermarking by modifying selected DWT-DCT coefficients," in IEEE Access, vol. 9, pp. 45474-45485, 2021.
- [3] H.B. Macit, "Mobil cihaz görüntüleri için entropi tabanlı kırılğan damgalama metodu geliştirilmesi," Ph.D. dissertation, Comput. Eng., Süleyman Demirel Univ., Isparta, Turkey, 2019.
- [4] D. Haueter, "Worldwide image capture forecast," Rise Above Research, pp. 2021 – 2026, 2022.

- [5] A.K. Abdulrahman and S. Öztürk, "A novel hybrid DCT and DWT based robust watermarking algorithm for color images," *Multimed. Tools and Appl.*, vol. 78, pp. 17027-17049, 2019.
- [6] J. Liu, J. Huang, Y. Luo, L. Cao, S. Yang, D. Wei and R. Zhou, "An optimized image watermarking method based on HD and SVD in DWT domain," in *IEEE Access*, vol. 7, pp. 80849-80860, 2019.
- [7] S. Kumar and B.K. Singh, "DWT based color image watermarking using maximum entropy," *Multimed. Tools and Appl.*, vol. 80, pp. 15487–15510, 2021.
- [8] A. Al-Haj, "Combined DWT-DCT digital image watermarking," *J. Comput. Sci.*, vol. 9, pp. 740-746, ISSN 1549-3636, 2007.
- [9] E.E. Hemdan, "An efficient and robust watermarking approach based on single value decompression, multi-level DWT, and wavelet fusion with scrambled medical images," *Multimed. Tools Appl.*, vol. 80, pp. 1749–1777, 2021.
- [10] C. Patvardhan, P. Kumar and C.V. Lakshmi, "Effective color image watermarking scheme using YCbCr color space and QR code," *Multimed. Tools Appl.*, vol.77, pp. 12655–12677, 2018.
- [11] M. Boreiry and M.R. Keyvanpour, "Classification of watermarking methods based on watermarking approaches," *Artif. Intell. Robot.*, Tehran, Iran, pp. 73-76, 2017.
- [12] C. Yin, L. Li, A. Lv and L. Qu, "Color image watermarking algorithm based on DWT-SVD," *Proc. IEEE Int. Conf. Automat. Logistics*, Jinan, China, August 18-21, 2007.
- [13] M. Patel, P.S. Sajja, R. Sheth, "Analysis and survey of digital watermarking techniques," *Int. J. Adv. Res. Comput. Sci. Softw. Eng.*, vol. 3, no. 10, pp. 203-210, 2013.
- [14] A. Abdülkhaev, "A new approach for video watermarking," M.S. thesis, *Elect. Electron. Eng.*, Gaziantep Univ., 66p, 2016.
- [15] C. Petzold, "Triple standard: three new video modes from IBM," *PC Magazine*, July 1987.
- [16] J. Richter, *Power programming the IBM XGA*, MIS Press, ISBN: 1-55828-127-4, 1992.
- [17] Digital Cinema Initiatives LLC, "Digital cinema system specification document (v.1.4.2)," 2022.
- [18] Digital cinema distribution master, SMPTE 428-1-2006, The Society of Motion Picture and Television Engineers, 2006.
- [19] Ultra-High Definition Television, Image Parameter Values for Program Production, SMPTE ST 2036-1:2014, Society of Motion Picture and Television Engineers, 2014.
- [20] D. Lee, "Apple announces \$4,999 Pro Display XDR,". [Online]. Available: <https://www.theverge.com/2019/6/3/18644791/apple-mac-pro-display-xdr-6k-retina-hdr-wwdc-2019>, 2019.
- [21] Parameter values for ultra-high definition television systems for production and international programme exchange, Rec. ITU-R BT.2020-2, International Telecommunication Union, Geneva, 2015.

- [22] D. Lokas, "Innolux premieres world's first 100 inch 16K display the best vision ever," DisplayDaily, [Online]. Available: <https://displaydaily.com/innolux-to-showcase-smartwatch-with-flexible-oled-display/>, 2018.
- [23] https://en.wikipedia.org/wiki/List_of_common_resolutions, Access date: 30.12.2022
- [24] Z. Wang, A.C. Bovik, H.R. Sheikh and E.P. Simoncelli, "Image quality assessment: From error visibility to structural similarity," IEEE Trans. Image Process., vol. 13, no. 4, pp. 600-612, 2004.
- [25] Z.H. Wei, P. Qin and Y.Q. Fu, "Perceptual digital watermark of images using wavelet transform," IEEE Trans. Consum. Electron., vol. 44, no. 4, pp. 1267-1272, Nov. 1998.
- [26] X. Yu, P. Dai, W. Li, L. Ma, "Towards efficient and scale-robust ultra-high-definition image demoreing," arXiv:2207.09935, 2022.
- [27] F. Kahlessenane, A. Khaldi, R. Kafi and S. Euschi, "A DWT based watermarking approach for medical image protection," J. Ambient Intell. Humanized Comput., vol. 12, pp. 2931-2938, 2021.
- [28] K.J. Giri, S.M.K. Quadri, R. Bashir and J.I. Bhat, "DWT based color image watermarking: a review," Multimed. Tools Appl., vol. 79, pp.32881-32895, 2020.
- [29] H.C. Huang, F.H. Wang and J.S. Pan, "Efficient and robust watermarking algorithm with vector quantization," Electron. Lett., vol. 37 no. 13, pp. 826-828, 2001.
- [30] C. Qin, P. Ji, J. Wang and C.C. Chang, "Fragile image watermarking scheme based on VQ index sharing and self-embedding," Multimed. Tools Appl., vol. 76, no. 2, pp. 2267-2287, 2017.
- [31] M. Barni, F. Bartolini, A.D. Rosa and A. Piva, "Color image watermarking in the Karhunen-Loeve transform domain," J. Electron. Imaging, vol. 11, no. 1, pp. 87-95, 2002.
- [32] M. Botta, D. Cavagnino, V. Pomponiu, "Fragile watermarking using Karhunen-Loeve transform: the KLT-F approach," Soft Comput., vol. 19, no. 7, pp. 1905-1919, 2015.
- [33] E. Etemad, S. Samavi, S.M.R. Soroushmehr, N. N. Karimi, M. Etemad, S. Shirani and K. Najarian, "Robust image watermarking scheme using bit-plane of hadamard coefficients," Multimed. Tools Appl., vol. 77, no. 2, pp. 2033-2055, 2018.
- [34] J. Li, C. Yu, B.B. Gupta and X. Ren, "Color image watermarking scheme based on quaternion Hadamard transform and Schur decomposition," Multimed. Tools Appl., vol. 77, no. 4, pp. 4545-4561, 2018.
- [35] L. Chen and J. Zhao, "Contourlet-based image and video watermarking robust to geometric attacks and compressions," Multimed. Tools Appl., vol. 77, no. 6, pp. 7187-7204, 2018.
- [36] Q. Su, G. Wang, G. Lv, X. Zhang, G. Deng and B. Chen, "A novel blind color image watermarking based on Contourlet transform and Hessenberg decomposition," Multimed. Tools Appl., vol. 76, no. 6, pp. 8781-8801, 2017.
- [37] D. Mistry and A. Banerjee, "Discrete wavelet transform using Matlab," Int. J. Computer Eng. Technol., vol. 4, no. 2, ISSN:0976-6375, pp. 252-259, 2013.
- [38] Ş. Doğan, "Yeni bir sayısal damgalama tekniği ile biyometrik uygulamalar," Ph.D. dissertation, Comput. Eng. Comput. Sci. Control, Firat Univ., Elazığ, Turkey, 2011.

- [39] K. Mahmoud, S. Datta and J. Flint, "Frequency domain watermarking: An overview," *Int. Arab J. Inf. Technol.*, vol. 2, no. 1, pp. 33-47, 2005.
- [40] P. Porwik, "The Haar-wavelet transform in digital image processing: Its status and achievements," *Mach. Graph. Vision*, vol. 13, no.1/2, pp. 79-98, 2004.
- [41] V. Santhi, N. Rekha and S. Tharini, "A hybrid block based watermarking algorithm using DWT-DCT-SVD techniques for color images," *Int. Conf. Comput., Commun. Netw.*, pp. 1-7, 2008.
- [42] O. Jane and E. Elbaşı, "A new approach of non-blind watermarking methods based on DWT and SVD via LU decomposition," *Turkish J. Electr. Eng. Comput. Sci.*, vol. 22, no. 5, pp. 1354-1366, 2014.
- [43] A. Mishra, C. Agarwal, A. Sharma and P. Bedi, "Optimized gray-scale image watermarking using DWT-SVD and firefly algorithm," *Expert Syst. Appl.*, vol. 41, no. 17, pp. 7858-7867, 2014.
- [44] M. Hsieh, D. Tseng and Y. Huang, "Hiding digital watermarks using multiresolution wavelet transform," *IEEE Trans. Ind. Electron.*, vol. 48, no. 5, pp. 875-882, 2001.
- [45] E. Yavuz, "Duruk imgelerde damgalama ve veri saklama," Ph.D. dissertation, *Elect. Electron. Eng.*, Ankara University, 2008.
- [46] A. Sverdlov, S. Dexter and A.M. Eskicioglu, "Robust DCT-SVD domain image watermarking for copyright protection: Embedding data in all frequency," presented at the 13th European Signal Processing Conference, Antalya, 2005.
- [47] D.R.I.M. Setiadi, "PSNR vs SSIM: imperceptibility quality assessment for image steganography," *Multimed. Tools Appl.*, vol. 80, pp. 8423-8444, 2021.
- [48] P.M. Naini, *Digital watermarking using Matlab, engineering education and research using Matlab*, Ali Assi, Ed., ISBN: 978-953-307-656-0, InTech, Iran, 2011.
- [49] E. Ganic and A.M. Eskicioğlu, A.M., "Robust DWT-SVD domain image watermarking: Embedding data in all frequencies," presented at the 6th Workshop Multimed. Secur., Magdeburg, Germany, September 20-21, 2004.
- [50] Y.S. Lee, Y.H. Seo and D.W. Kim, "Blind image watermarking based on adaptive data spreading in n-Level DWT subbands," *Hindawi Secur. Commun. Netw.*, 2019.
- [51] N.V. Dharwadkar, B.B. Amberker and A. Gorai, "Non-blind watermarking scheme for color images in RGB space using DWT-SVD," 2011 presented at the *Int. Conf. Commun. Signal Process.*, Kerala, India, pp. 489-493, 2011.
- [52] S. P. Sathya and S. Ramakrishnan, "Fibonacci based key frame selection and scrambling for video watermarking in DWT-SVD domain," *Wireless Pers. Commun.*, vol. 102, pp. 2011-2031, 2018.
- [53] Z. Zhang, C. Wang and X. Zhou, "Image watermarking scheme based on Arnold transform and DWT-DCT-SVD," presented at the *IEEE 13th Int. Conf. Signal Proc.*, Chengdu, China, pp. 805-810, 2016.